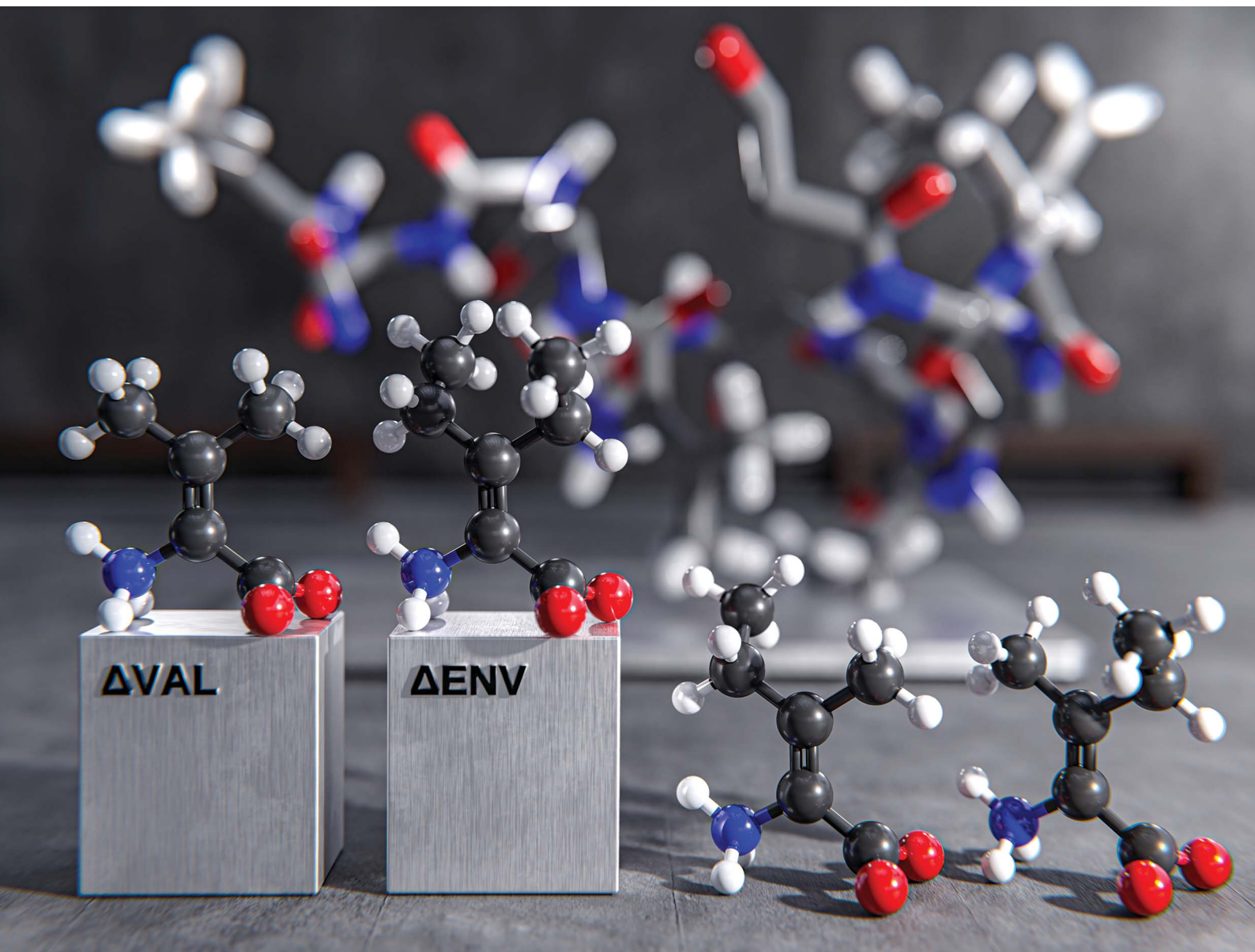


Chemical Science

Volume 13
Number 7
21 February 2022
Pages 1837–2138

rsc.li/chemical-science



ISSN 2041-6539

Cite this: *Chem. Sci.*, 2022, 13, 1899

All publication charges for this article have been paid for by the Royal Society of Chemistry

Synthesis and evaluation of potent yaku'amide A analogs†

Concordia C. L. Lo,^a Daniel Joaquin,^a Diego A. Moyá,^a Alexander Ramos,^a David W. Kastner,^a Stephen M. White,^a Blake L. Christensen,^a Joseph G. Naglich,^b William J. Degnen^c and Steven L. Castle^{*,a}

Two full-length analogs of the anticancer peptide yaku'amide A (**1a**) and four partial structures have been synthesized. These analogs were identified by computational studies in which the three *E*- and *Z*- Δ Ile residues of the natural product were replaced by the more accessible dehydroamino acids Δ Val and Δ Env. Of the eight possible analogs, modeling showed that the targeted structures **2a** and **2b** most closely resembled the three-dimensional structure of **1a**. Synthesis of **2a** and **2b** followed a convergent route that was streamlined by the absence of Δ Ile in the targets. Screening of the compounds against various cancer cell lines revealed that **2a** and **2b** mimic the potent anticancer activity of **1a**, thereby validating the computational studies.

Received 31st October 2021
Accepted 2nd January 2022

DOI: 10.1039/d1sc05992k

rsc.li/chemical-science

Introduction

The linear peptide yaku'amide A (**1a**, Fig. 1) was isolated by Matsunaga and co-workers from the deep-sea sponge *Ceratospongia* sp.¹ It contains several unusual β -*tert*-hydroxy amino acids (β -OHAAs) and tetrasubstituted dehydroamino acids (Δ AAAs). It strongly inhibits the growth of P388 murine leukemia cells (IC₅₀ = 14 ng mL⁻¹) and has exhibited a unique activity profile when screened against the JFCR39 cancer cell line panel.¹ These data suggest that **1a** functions *via* a mode of action that is distinct from other anticancer agents.

Yaku'amide A and its close relative yaku'amide B (**1b**, Fig. 1) have attracted attention by virtue of their singular structural features, intriguing bioactivity, and scarcity in nature. In 2013, Inoue and co-workers synthesized the originally proposed structure of **1a** and assigned the configuration of its *N*-terminal acyl subunit (NTA).^{2a} Then, while constructing **1b** they determined that the structures of both yaku'amides had been misassigned. Their meticulous efforts resulted in the first total syntheses of the yaku'amides and established that the configurations of four residues (*D*- and *L*- β -OHVal, *D*- and *L*-Val) had been transposed.^{2b} Inoue and co-workers later discovered that **1b** reduces cellular ATP levels by simultaneously inhibiting ATP synthesis and promoting ATP hydrolysis through binding to the complex mitochondrial enzyme F₀F₁-ATP synthase.^{2c} Recently,

they have devised a solid-phase synthesis of **1b** (ref. 3a) and demonstrated that the *E/Z* stereochemistry of the Δ Ile residues modulates its anticancer activity.^{3b}

Inoue's groundbreaking total syntheses of **1a** and **1b** illustrate the challenges inherent in constructing unsymmetrical tetrasubstituted Δ AAAs such as *E*- and *Z*- Δ Ile. These residues readily isomerize *via* azlactone intermediates when activated for peptide couplings.⁴ To prevent *E/Z* isomerization, Inoue and co-workers initially resorted to a lengthy sequence of reactions involving backbone amide protection that was required for each of the three Δ Ile residues present in **1a** and **1b**.² They subsequently streamlined this sequence^{3a} and eliminated the need for backbone protection,^{3b} but specialized and air-sensitive building blocks are necessary to execute the required Staudinger ligations. In our recent total synthesis of **1a**, we devised a one-pot process involving *anti* dehydration, azide reduction, and O \rightarrow N acyl transfer to forge the Δ Ile residues and generate amide bonds at their *C*-termini without recourse to backbone amide protection or synthetically challenging building blocks.⁵ This strategy thwarted *E/Z* isomerization and enabled an efficient route to yaku'amide A, but our synthesis was still too lengthy to produce sufficient quantities of the natural product for in-depth studies of its mode of action.

We closely examined the structure of **1a** in order to identify more accessible analogs that would retain its shape and presumably its bioactivity. While the three synthetically challenging Δ Ile residues were strong candidates for removal, we postulated that they play a critical role in establishing the three-dimensional structure of **1a**. Their low-energy conformations are likely limited in number by the high levels of A_{1,3}-strain that are characteristic of tetrasubstituted alkenes. This phenomenon should confer a rigid and well-defined structure⁶ on

^aDepartment of Chemistry and Biochemistry, Brigham Young University, Provo, UT 84602, USA. E-mail: scastle@chem.byu.edu

^bBristol Myers Squibb, Research & Early Development, Mechanistic Pharmacology-Leads Discovery & Optimization, Rte 206 & Province Line Rd, Princeton, NJ 08543, USA

^cSpectrix Analytical Services, USA

† Electronic supplementary information (ESI) available. See DOI: 10.1039/d1sc05992k



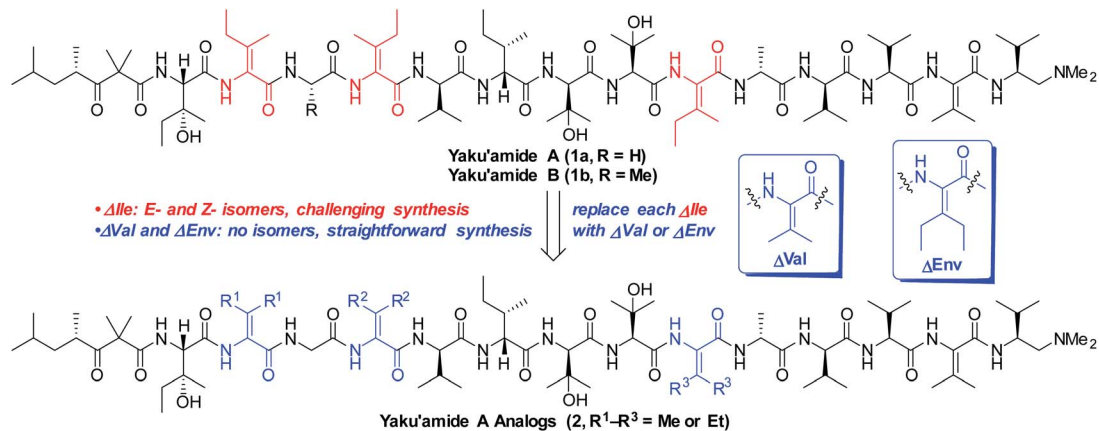


Fig. 1 Yaku'amide A and analogs containing symmetrical bulky ΔAAs.

yaku'amide A. Accordingly, we deemed it necessary to retain bulky ΔAAs in designed analogs of **1a**.

In contrast to ΔIle, the symmetrical bulky ΔAAs dehydrovaline and dehydroethylnorvaline (ΔVal and ΔEnv, Fig. 1) are easier to construct due to their lack of geometrical isomers. Since they approximate the size of ΔIle, we reasoned that they could be surrogates for the three ΔIle residues present in yaku'amide A. The resulting analogs could be synthesized in significantly fewer steps than the natural product and should be useful tools for probing its mode of action by virtue of closely resembling its three-dimensional shape. Herein, we report the computationally-guided design and synthesis of two full-length yaku'amide A analogs containing ΔVal and ΔEnv in place of ΔIle along with the evaluation of their anticancer properties. We also investigated the bioactivity of key yaku'amide A partial structures.

Results and discussion

We recognized that replacing each of the three ΔIle residues of **1a** with either ΔVal or ΔEnv would result in a total of eight possible full-length analogs. We turned to computational chemistry to determine which of these compounds would most closely resemble the three-dimensional structure of the natural product. To approximate **1a** and its analogs, we employed the ONIOM⁷ QM:MM method as implemented in Gaussian 09,⁸ which divides the system of interest into three layers: high, medium, and low. The high layer is treated with the most accurate method and the low layer is treated with a computationally cheaper method. Using ONIOM, we divided **1a** and each potential analog into high and low layers, which were treated with quantum mechanics (QM) and molecular mechanics (MM), respectively. We employed the B3LYP 6-311g(d,p) basis set⁹ for the QM region comprised of the dehydroamino acids, and we treated all other amino acids using MM with the AMBER96 force field.¹⁰ The partial charges for all nonstandard residues in the MM region were assigned using R.E.D. tools,¹¹ and the harmonic stretch, bond, and torsional angle parameters were generated with AMBER tools.¹² We computed the final structures in a dielectric continuum treated with the IEF-PCM solvation model to approximate the effects of water.¹³

Each analog of **1a** was assigned a three-letter abbreviation, where E represents ΔEnv and V represents ΔVal. Each letter signifies a residue replacing a ΔIle residue of **1a**, with the substitutions listed in order from the *N*- to the *C*-terminus. We used the optimized structures of these eight compounds to calculate two separate root mean square deviation (RMSD) values *via* the VMD software¹⁴ by aligning the structure of **1a** with that of each analog using either the backbone atoms (Fig. 2A) or all heavy atoms common to both molecules being compared (Fig. 2B). Performing two separate RMSD calculations was advantageous because the relative impact of the backbone orientation *versus* that of the side chains on the bioactivity of **1a** is unknown. As expected, the RMSD calculations that included all common heavy atoms produced higher values due to the greater flexibility of the side chains relative to the backbone. Of the eight possible analogs, EVV (hereafter known as **2a**) best conserved the three-dimensional structure of yaku'amide A (Fig. 2 and 3).¹⁵ Compound VEV (hereafter known as **2b**) was selected as the second-best analog of **1a** (Fig. 2).

Our strategy for synthesizing **1a** (ref. 5) could be readily adapted to access the two targeted analogs, as shown in the retrosynthetic analysis that is summarized in Scheme 1. Disconnection of the target compounds at the indicated amide

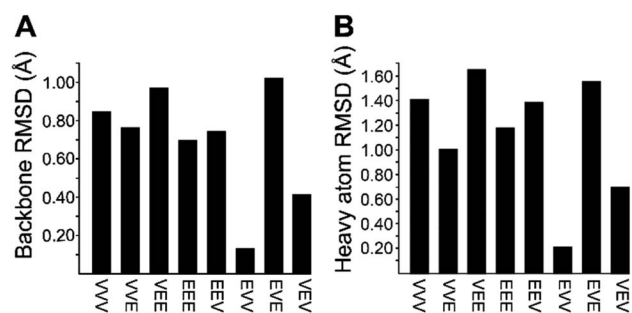


Fig. 2 RMSD values generated by (A) superimposing the backbone atoms of **1a** on each of its eight possible analogs, and by (B) accounting for the differences between ΔIle, ΔVal, and ΔEnv by superimposing all heavy atoms (backbone and side chain) common to **1a** and each analog.



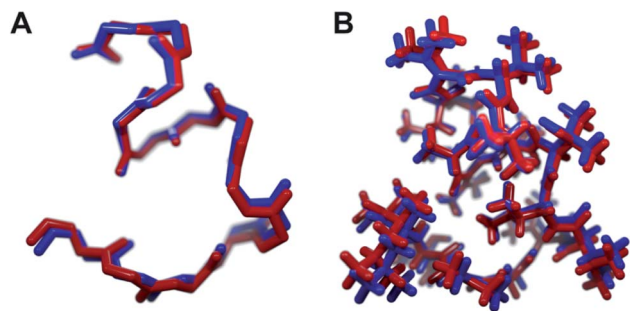
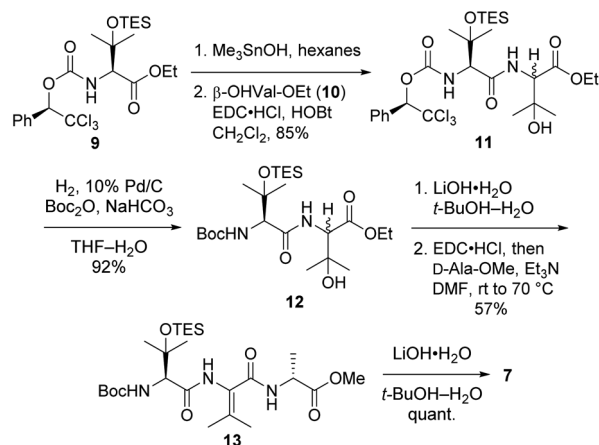


Fig. 3 The minimized structures of **1a** and **2a** superimposed showing (A) only the backbone atoms, or (B) all atoms common to both compounds.

bonds revealed four subunits: an *N*-terminal acyl group (**3**) and a right-hand nonapeptide (**5**) common to **2a** and **2b** along with two different left-hand pentapeptides **4a** and **4b**. The nonapeptide was then dissected into dipeptide **6**, tripeptide **7**, and tetrapeptide **8**. Intermediates **3**, **6**, and **8** were all employed in our total synthesis of **1a**, so this plan only required three new subunits: **7**, **4a**, and **4b**. These fragments would likely be much easier to construct than the corresponding intermediates used in our yaku'amide A total synthesis owing to the replacement of each native Δ Ile residue with either Δ Val or Δ Env.

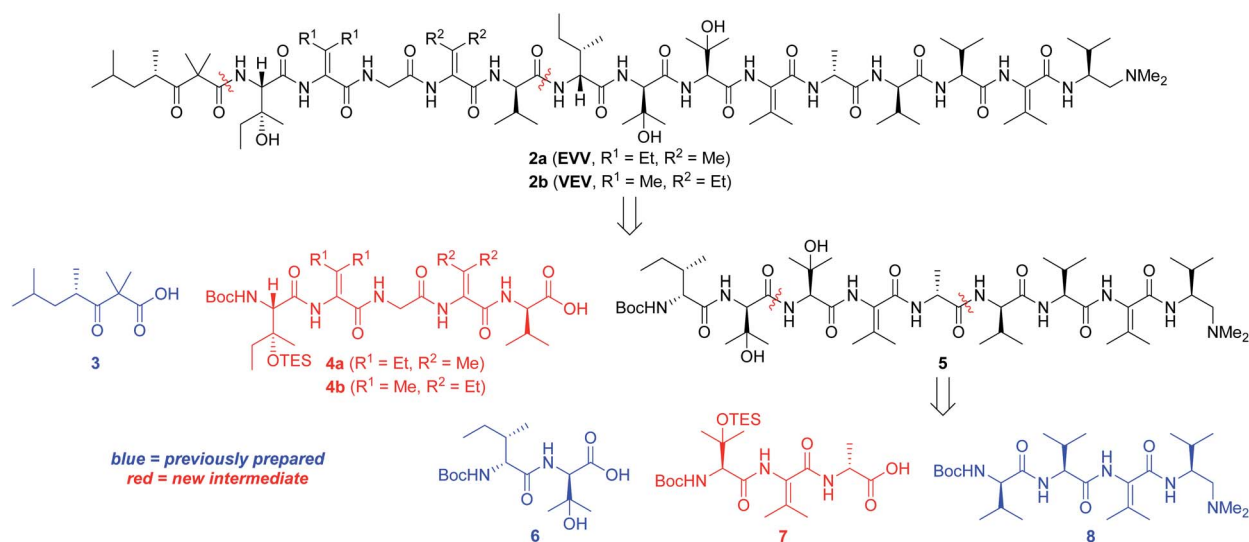
Tripeptide **7**, which is common to both **2a** and **2b**, was prepared as outlined in Scheme 2. Saponification of *L*- β -OHVal derivative **9** (ref. 5) required Me_3SnOH ¹⁶ due to the sensitivity of its chiral carbamate moiety to bases that are commonly used to hydrolyze esters. Coupling of the resulting acid to racemic β -OHVal-OEt (**10**)^{5,17} furnished dipeptide **11** as a mixture of diastereomers. Hydrogenolysis of **11** in the presence of Boc_2O cleaved the trichloromethylated benzyl carbamate and replaced it with a Boc group. Concomitant scission of the TES ether was prevented by including NaHCO_3 in the reaction mixture. The resulting dipeptide **12** was saponified under standard



Scheme 2 Synthesis of tripeptide **7**.

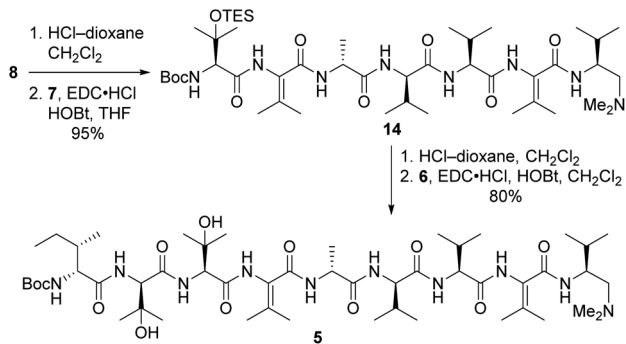
conditions, and the crude acid was subjected to the one-pot dehydration–amidation protocol that we devised for the synthesis of **1a**.⁵ First, exposure of the acid to $\text{EDC}\cdot\text{HCl}$ served to dehydrate the tertiary alcohol and activate the carboxylate, triggering cyclization to form an azlactone. Then, addition of *D*-Ala-OMe and Et_3N along with heating of the reaction mixture facilitated azlactone ring-opening and delivered Δ Val-containing tripeptide **13**. Notably, the dehydration step caused both epimers of **12** to converge to a single alkene product. Finally, saponification of **13** afforded the key tripeptide acid **7**.

Tripeptide **7** was combined with the previously constructed subunits **6** and **8** (ref. 5) to furnish nonapeptide **5** as depicted in Scheme 3. Acidic removal of the Boc moiety from tetrapeptide **8** and subsequent coupling to **7** delivered heptapeptide **14** in excellent yield. Then, exposure of **14** to HCl simultaneously cleaved the Boc and TES groups from its *N*-terminal *L*- β -OHVal residue. Coupling of the resulting crude amine with dipeptide **6** afforded nonapeptide **5** in good yield. HPLC analysis of the



Scheme 1 Retrosynthesis of yaku'amide A analogs.

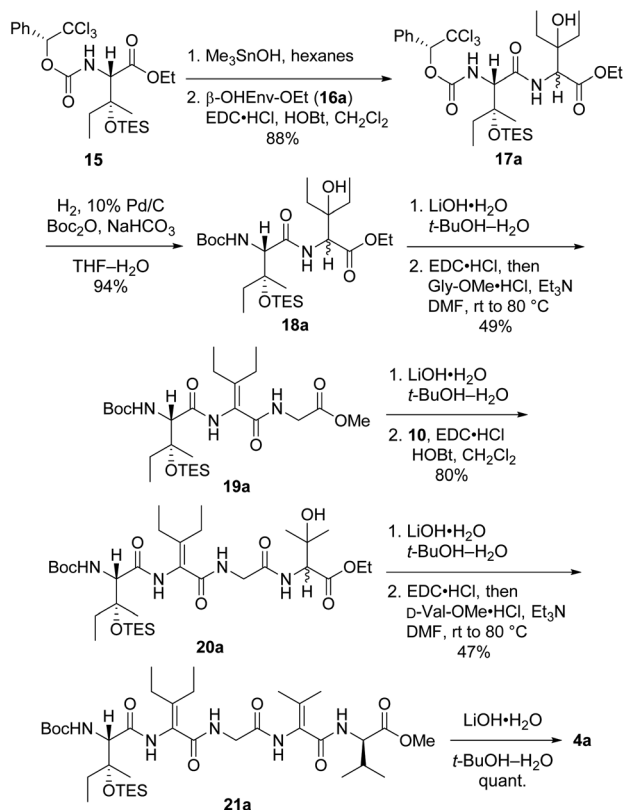




Scheme 3 Synthesis of nonapeptide 5.

heptapeptide and nonapeptide did not reveal any evidence of epimerization in the fragment couplings.

Synthesis of first-choice analog **2a** required pentapeptide **4a**, which was constructed as shown in Scheme 4. Me_3SnOH -mediated hydrolysis of β -OH-ILE derivative **15** (ref. 5) was followed by coupling of the crude carboxylic acid to racemic β -OHEnv-OEt (**16a**),¹⁸ delivering dipeptide **17a** as a mixture of diastereomers. Swapping the chiral carbamate for a Boc group then furnished **18a** in excellent yield. Saponification and subsequent dehydration–amidation with Gly-OMe were challenging due to the hindered C-terminal residue. Thus, a slightly lower yield was obtained relative to the dehydration–amidation of dipeptide **12** depicted in Scheme 2. The remaining amino

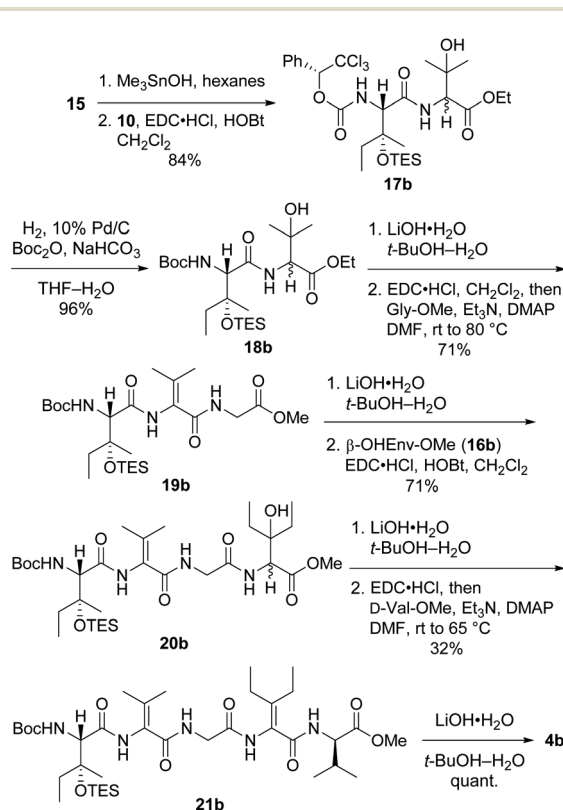


Scheme 4 Synthesis of pentapeptide 4a.

acids Δ Val and D-Val were attached to **19a** via a similar sequence involving coupling followed by one-pot dehydration–amidation. Saponification of the resulting pentapeptide **21a** revealed carboxylic acid **4a**.

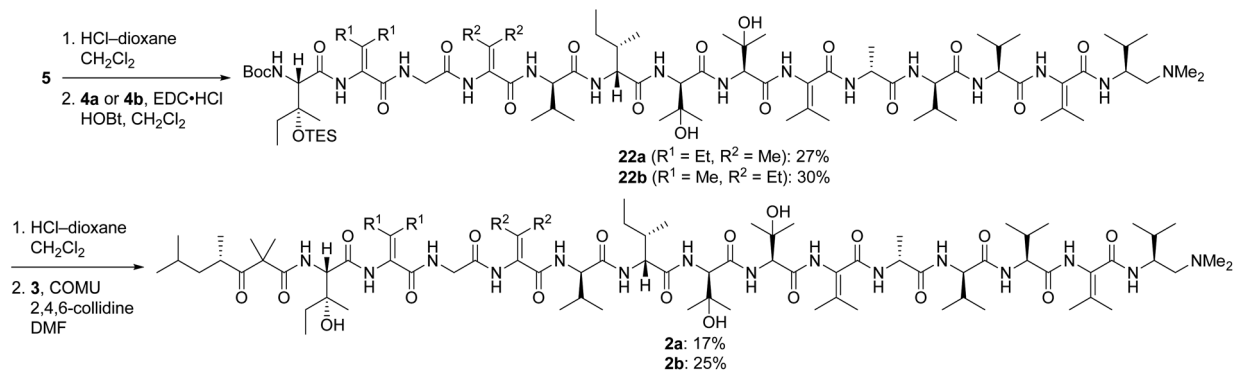
Preparation of pentapeptide **4b** required for the second-choice analog **2b** resembled the construction of **4a** shown above with a few key exceptions that are presented in Scheme 5. Conversion of dipeptide **18b** into Δ Val-containing tripeptide **19b** was most readily accomplished with DMAP as an additive to promote ring-opening amidation of the azlactone intermediate. The high yield of this process relative to analogous transformations in the syntheses of **7** (see Scheme 2) and **4a** (see Scheme 4) is likely due to the use of less hindered coupling partners (Δ Val and Gly). Conversely, formation of pentapeptide **21b** involved the lowest-yielding dehydration–amidation sequence owing to the highly hindered Δ Env and D-Val coupling partners. This process was further complicated by retro aldol scission of the β -OHEnv residue during saponification of tetrapeptide **20b**. Utilizing methyl ester **16b** (ref. 19) instead of ethyl ester **16a** that was employed in synthesizing **4a** mitigated but did not eliminate this problem.

Pentapeptides **4a** and **4b** were coupled with the free amine derived from nonapeptide **5** and elaborated into the targeted analogs **2a** and **2b** as illustrated in Scheme 6. Although the deprotection and coupling conditions were identical to those employed in the total synthesis of yaku'amide A,^{2,5} lower yields were obtained in the current reactions. Apparently, the subtle structural differences between the building blocks employed in



Scheme 5 Synthesis of pentapeptide 4b.



Scheme 6 Completion of the syntheses of **2a** and **2b**.

the total synthesis and those used in the current study impacts the yields of these late-stage peptide couplings. Fortunately, ample quantities of **5**, **4a**, and **4b** were available, allowing us to produce **2a** and **2b** in amounts sufficient for evaluation of their anticancer activity. Thus, optimization of the final two peptide couplings was deemed unnecessary.

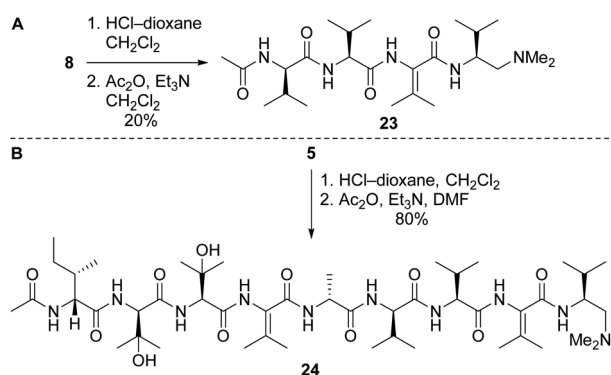
Our route to **2a** and **2b** provided access to partial structures that could be used to determine if the pharmacophore of the yaku'amides is localized to a single region of the molecules or if the full-length structures are required for bioactivity. Right-hand and central-right partial structures **23** and **24** were easily obtained by acetylation of the previously prepared tetrapeptide **8** and nonapeptide **5**, respectively (Scheme 7). We elected not to optimize the acetylation of **8**, as the abundance of this tetrapeptide enabled us to prepare the requisite amounts of **23** despite the low yield. We were pleased to discover that acetylation of **5** was high-yielding.

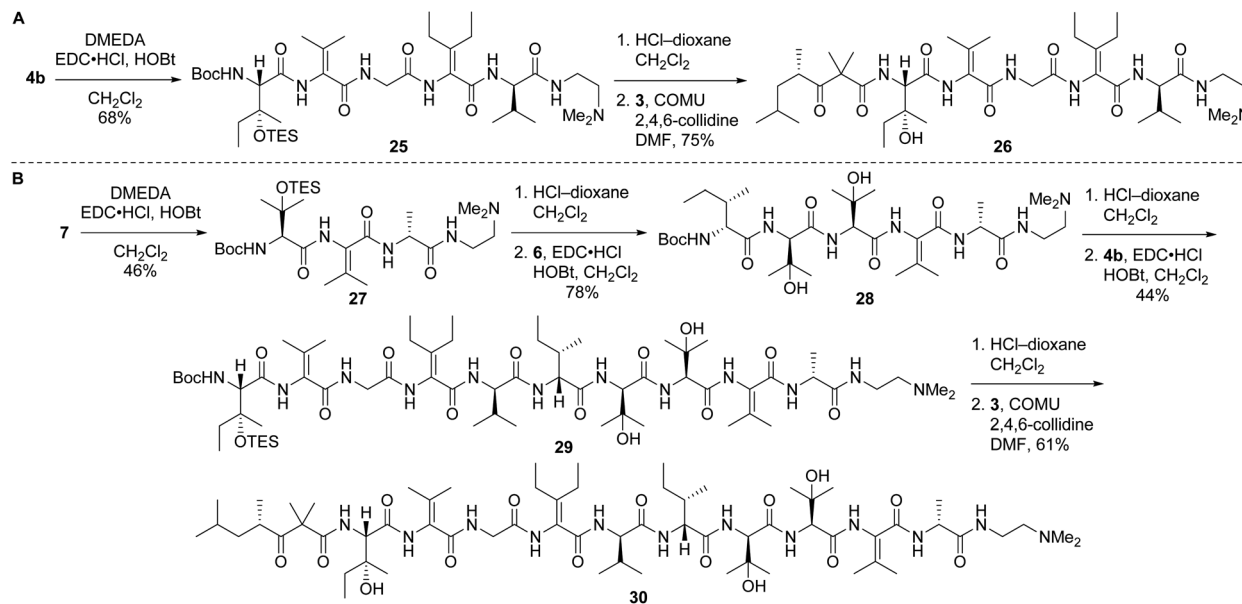
Left-hand and left-central partial structures **26** and **30** were constructed as outlined in Scheme 8. Capping of pentapeptide **4b** with *N,N*-dimethylethylenediamine (DMEDA, a simplified version of the *C*-terminal amino moiety present in yaku'amide A and its full-length analogs) furnished **25** in good yield. Then, HCl-mediated cleavage of the Boc and TES groups followed by coupling of the resulting primary amine with acid **3** delivered left-hand partial structure **26**. Preparation of the left-central

partial structure commenced with the high-yielding union of DMEDA-capped tripeptide **27** and dipeptide **6**. Boc deprotection of the resulting central fragment **28** and subsequent coupling with **4b** afforded **29** in moderate yield. Acidic deprotection of this intermediate and coupling with **3** proceeded smoothly to produce the targeted partial structure **30**.

Inoue and co-workers recently observed slow retro-aldol reactions of unnatural *E/Z* isomers of yaku'amides upon storage in the presence of dilute acetic acid.²⁰ This cleavage occurs at the β -OH residues that are adjacent to the Δ AAs and is presumably the result of increased steric hindrance (*i.e.*, $A_{1,3}$ strain) caused by the unnatural alkene isomers. We did not observe retro-aldol scission of any of our yaku'amide A full-length analogs or partial structures; however, we did not expose them to dilute acetic acid for prolonged periods of time. Thus, it is possible that our compounds would exhibit the same lability as Inoue's compounds under similar storage conditions.

The antiproliferative activity profiles of **1a**, its full-length analogs **2a** and **2b**, and its partial structures (**23**, **24**, **26**, and **30**) were determined by *in vitro* screening in 72 hours MTS cell proliferation assays against a panel of 18 different human cancer cell lines. The partial structures were essentially inactive ($IC_{50} > 25 \mu M$ in almost all cases),²¹ suggesting that the entire sequence of yaku'amide A is required for its bioactivity. Apart from the MCF7 cell line in which only **1a** was potent, both **2a** and **2b** exhibited a similar pattern of activity to yaku'amide A, demonstrating their suitability as mimics of the natural product (Fig. 4). All three peptides were potent inhibitors of the A549, MV411, OVCAR3, HL60, and SNUC1 cell lines ($IC_{50} = 50$ – 250 nM). Analog **2a** displayed increased potency (*ca.* 2–4-fold) compared to **2b** against most of the cell lines, and its activity profile was more similar to that of the natural product. These results are consistent with our original prediction that **2a** would mimic the three-dimensional structure of **1a** more closely than **2b**. The three peptides were also evaluated for their antiproliferative activity against the lung fibroblast MRC5 cell line. The encouraging lack of potency against these noncancerous cells suggests that yaku'amide A and related analogs possess a satisfactory therapeutic window for use as anticancer agents.

Scheme 7 Syntheses of partial structures **23** (right) and **24** (central-right).



Scheme 8 Syntheses of partial structures 26 (left) and 30 (left-central).

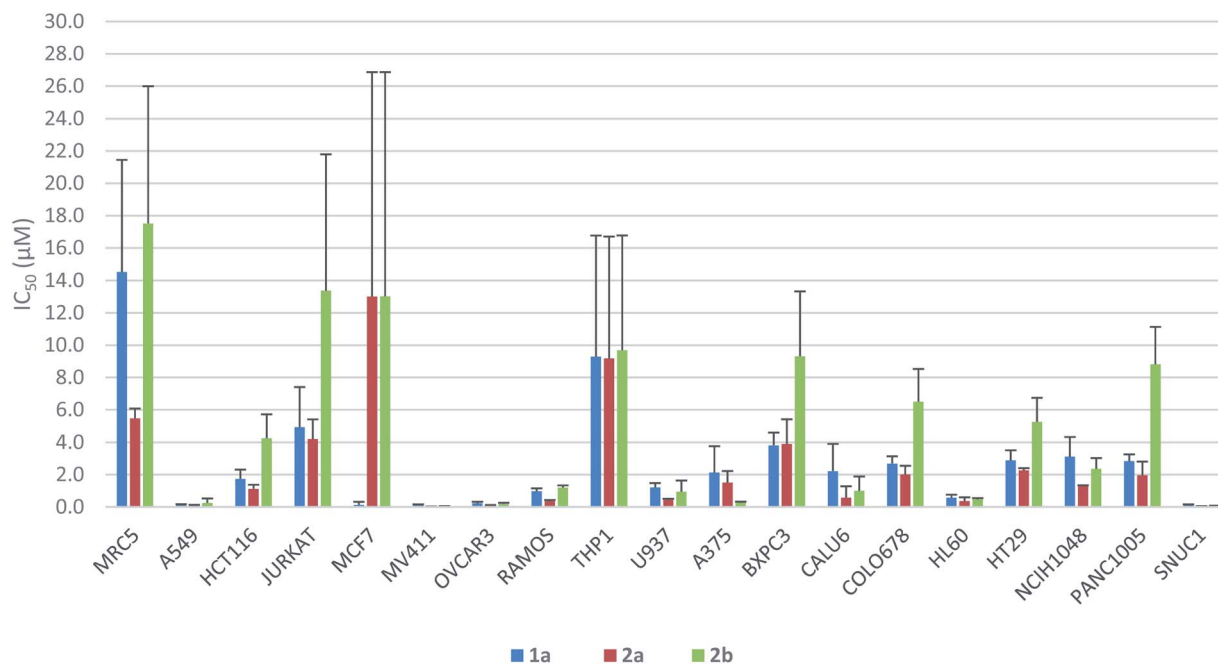


Fig. 4 Antiproliferative activity profiles of 1a and its full-length analogs 2a and 2b.

Conclusions

In an attempt to identify synthetically accessible full-length analogs of the potent anticancer peptide yaku'amide A, we performed computational studies in which its *E*- and *Z*- Δ Ile residues were replaced by the symmetrical bulky Δ AAAs Δ Val and Δ Env. Of the eight candidate structures, EVV (2a) and VEV (2b) emerged as promising mimics of the natural product. We then synthesized these peptides *via* a convergent route modelled on our total synthesis of 1a. Replacement of the somewhat

cumbersome chemistry required to install *E*- and *Z*-Ile by the straightforward one-pot dehydration–amidation suitable for generating Δ Val and Δ Env streamlined the syntheses of key intermediates. Although the final peptide couplings were low-yielding, the abundance of key intermediates 5, 4a, and 4b due to their efficient construction allowed us to overcome this obstacle and prepare sufficient 2a and 2b to perform anticancer assays. Our syntheses of these full-length yaku'amide A analogs also provided access to four partial structures of the natural product.



Bioassays revealed that both **2a** (EVV) and **2b** (VEV) mimic the anticancer activity profile of **1a**. Thus, these accessible analogs should be useful probes of the intriguing mode of action of the yaku'amides.^{2c} The data shown in Fig. 4 demonstrate that **2a** more closely imitated the anticancer activity of **1a** than did **2b**. This result is consistent with our computationally derived hypothesis that **2a** would serve as the best mimic of the three-dimensional structure of **1a**. Importantly, this result provides some validation for our computational methods and suggests that they could be employed to design potent analogs of other complex bioactive peptides.

Data availability

All experimental procedures, spectral data, bioassay data, and computational data are available in the ESI†

Author contributions

S. L. C. devised the project, with C. C. L. L. and D. W. K. providing critical input. D. W. K. performed the computational studies. C. C. L. L., D. J., D. A. M., A. R., S. M. W., and B. L. C. synthesized the analogs and partial structures. J. G. N. and W. J. D. performed the anticancer assays. S. L. C. wrote the manuscript with contributions from all authors.

Conflicts of interest

There are no conflicts to declare.

Acknowledgements

We thank the National Institutes of Health (R15GM114789 and R15GM114789-S1) and Brigham Young University (Graduate Mentoring Award and Telford and Frank Woolley Memorial Award to C. C. L. L.; Simmons Center for Cancer Research Fellowships to C. C. L. L., D. A. M., D. J., and D. W. K.; Undergraduate Research Awards to D. W. K., S. M. W., and B. L. C.) for support. We also thank Courtney K. Dawes for assistance with the preparation of starting materials and the Bristol Myers Squibb compound management and cell technology teams for their efforts and support.

Notes and references

- R. Ueoka, Y. Ise, S. Ohtsuka, S. Okada, T. Yamori and S. Matsunaga, *J. Am. Chem. Soc.*, 2010, **132**, 17692.
- (a) T. Kuranaga, Y. Sesoko, K. Sakata, N. Maeda, A. Hayata and M. Inoue, *J. Am. Chem. Soc.*, 2013, **135**, 5467; (b) T. Kuranaga, H. Mutoh, Y. Sesoko, T. Goto, S. Matsunaga and M. Inoue, *J. Am. Chem. Soc.*, 2015, **137**, 9443; (c) K. Kitamura, H. Itoh, K. Sakurai, S. Dan and M. Inoue, *J. Am. Chem. Soc.*, 2018, **140**, 12189.
- (a) H. Itoh, K. Miura, K. Kamiya, T. Yamashita and M. Inoue, *Angew. Chem., Int. Ed.*, 2020, **59**, 4564; (b) K. Kamiya, K. Miura, H. Itoh and M. Inoue, *Chem.–Eur. J.*, 2021, **27**, 1088.
- (a) M. M. Stohlmeyer, H. Tanaka and T. J. Wandless, *J. Am. Chem. Soc.*, 1999, **121**, 6100; (b) J. S. Grimley, A. M. Sawayama, H. Tanaka, M. M. Stohlmeyer, T. F. Woiwode and T. J. Wandless, *Angew. Chem., Int. Ed.*, 2007, **46**, 8157; (c) N. Shangguan and M. Joullié, *Tetrahedron Lett.*, 2009, **50**, 6748.
- Y. Cai, Z. Ma, J. Jiang, C. C. L. Lo, S. Luo, A. Jalan, J. M. Cardon, A. Ramos, D. A. Moyá, D. Joaquin and S. L. Castle, *Angew. Chem., Int. Ed.*, 2021, **60**, 5162.
- A. Jalan, D. W. Kastner, K. G. I. Webber, M. S. Smith, J. L. Price and S. L. Castle, *Org. Lett.*, 2017, **19**, 5190.
- (a) S. Dapprich, I. Komiro, K. S. Byun, K. Morokuma and M. J. Frisch, *J. Mol. Struct.: THEOCHEM*, 1999, **461–462**, 1; (b) T. Vreven, K. S. Byun, I. Komaromi, S. Dapprich, J. A. Montgomery Jr, K. Morokuma and M. J. Frisch, *J. Chem. Theory Comput.*, 2006, **2**, 815.
- M. J. Frisch, *et al.*, *Gaussian 09*, Gaussian, Inc., Wallingford, CT, 2010.
- (a) J. A. Plumley and J. J. Dannenberg, *J. Comput. Chem.*, 2011, **32**, 1519; (b) Y. K. Kang and B. J. Byun, *J. Comput. Chem.*, 2010, **31**, 2915; (c) A. D. Becke, *J. Chem. Phys.*, 1993, **98**, 5648; (d) A. D. Becke, *J. Chem. Phys.*, 1993, **98**, 1372; (e) C. T. Lee, W. T. Yang and R. G. Parr, *Phys. Rev. B: Condens. Matter Mater. Phys.*, 1988, **37**, 785.
- W. D. Cornell, P. Cieplak, C. I. Bayly, I. R. Gould, K. M. Merz Jr, D. M. Ferguson, D. C. Spellmeyer, T. Fox, J. W. Caldwell and P. A. Kollman, *J. Am. Chem. Soc.*, 1995, **117**, 5179.
- F.-Y. Dupradeau, A. Pigache, T. Zaffran, C. Savineau, R. Lelong, N. Grivel, D. Lelong, W. Rosanski and P. Cieplak, *Phys. Chem. Chem. Phys.*, 2010, **12**, 7821.
- D. A. Case, *et al.*, *AMBER 2018*, University of California, San Francisco, 2018.
- (a) M. Cossi, V. Barone, R. Cammi and J. Tomasi, *Chem. Phys. Lett.*, 1996, **255**, 327; (b) E. Cancès, B. Mennucci and J. Tomasi, *J. Chem. Phys.*, 1997, **107**, 3032; (c) J. Tomasi, B. Mennucci and R. Cammi, *Chem. Rev.*, 2005, **105**, 2999.
- (a) W. Humphrey, A. Dalke and K. Schulten, *J. Mol. Graphics*, 1996, **14**, 33; (b) <http://www.ks.uiuc.edu/Research/vmd/>.
- J. A. Durrant, *Bioinformatics*, 2019, **35**, 2323.
- K. C. Nicolaou, M. Nevalainen, M. Zak, S. Bulat, M. Bella and B. S. Safina, *Angew. Chem., Int. Ed.*, 2003, **42**, 3418.
- Z. Ma, B. C. Naylor, B. M. Loertscher, D. D. Hafen, J. M. Li and S. L. Castle, *J. Org. Chem.*, 2012, **77**, 1208.
- J. Jiang, S. Luo and S. L. Castle, *Tetrahedron Lett.*, 2015, **56**, 3311.
- Compound **16b** was prepared by the same procedure used to synthesize known compound **16a** (see ref. 18 and ESI†).
- K. Kamiya, H. Itoh and M. Inoue, *J. Nat. Prod.*, 2021, **84**, 1854.
- Please see ESI† for the complete screening data set.

